

The ECMWF model climate: Recent progress through improved physical parametrizations

T. Jung, G. Balsamo, P. Bechtold,
A. Beljaars, M. Köhler¹, M. Miller,
J.-J. Morcrette, A. Orr², M. Rodwell and
A. Tompkins³

Research Department

¹ Current affiliation: DWD, Offenbach, Germany

² Current affiliation: BAS, Cambridge, United Kingdom

³ Current affiliation: ICTP/ESP, Trieste, Italy

Accepted for publication in Quart. J. Roy. Meteor. Soc.

April 2010

*This paper has not been published and should be regarded as an Internal Report from ECMWF.
Permission to quote from it should be obtained from the ECMWF.*



Series: ECMWF Technical Memoranda

A full list of ECMWF Publications can be found on our web site under:

<http://www.ecmwf.int/publications/>

Contact: library@ecmwf.int

©Copyright 2010

European Centre for Medium-Range Weather Forecasts
Shinfield Park, Reading, RG2 9AX, England

Literary and scientific copyrights belong to ECMWF and are reserved in all countries. This publication is not to be reprinted or translated in whole or in part without the written permission of the Director. Appropriate non-commercial use will normally be granted under the condition that reference is made to ECMWF.

The information within this publication is given in good faith and considered to be true, but ECMWF accepts no liability for error, omission and for loss or damage arising from its use.

Abstract

The progress achieved since 2005 in simulating today's climate with the European Centre for Medium-Range Weather Forecasts (ECMWF) model through improved physical parametrizations is described. Results are based on climate integrations at an intermediate horizontal resolution (T_L159) using major model versions employed operationally at ECMWF since June 2005. Recent improvements to the physical parametrization package are shown to substantially reduce long-standing systematic model deficiencies in the tropical precipitation, convectively coupled tropical waves, and circulation features in the Northern Hemisphere extratropics including synoptic-scale variability and Euro-Atlantic blocking. The climate integrations are augmented by a set of monthly forecast experiments. By considering the atmospheric response in a seamless sense, that is, from time-scales of hours to many months, an attempt is made to understand the impact of changes to the convection and radiation schemes. Overall, the largest and mostly beneficial impact results from the introduction of a major revision to the convection scheme made in November 2007. This is true for systematic errors in the tropics and extratropics over a wide range of timescales as well as for the short-range and medium-range deterministic forecast skill over the Northern Hemisphere.

1 Introduction

A frequently asked question is how well state-of-the-art atmospheric models simulate today's climate and how systematic errors have changed in time though improvements in model formulation (e.g., Jung 2005, Reichler and Kim 2008). An assessment of three generations of coupled models by Reichler and Kim (2008) shows that atmospheric components of state-of-the-art models are certainly not perfect but better than their predecessors. The authors explain this in terms of improvements in physical parametrizations and increased horizontal and vertical resolution.

A comprehensive study of systematic errors in the ECMWF model and their evolution from the 1980s has been presented by Jung and Tompkins (2003) and Jung (2005). These studies reveal substantial systematic error reduction in the medium-range (about 3–10 days), particularly during the 1980s and 1990s. However, even the model versions used in the early 2000s produced still substantial systematic errors beyond the medium-range such as an underestimation of synoptic activity in high-latitudes, underestimation of the frequency of occurrence of Euro-Atlantic blocking, a strong anti-cyclonic circulation bias in the North Pacific and short-comings in the tropical hydrological cycle.

In the meantime considerable effort at ECMWF has been devoted to improve the physical parametrization package in order to reduce the above-mentioned model problems. The aim of this study is to give an overview of the physical parametrization updates introduced since June 2005 and to describe, and where possible understand, their impact on the climate of the ECMWF model. As it turns out, recent improvements have been mostly beneficial in terms of alleviating some of the long-standing problems found in the ECMWF model (and more generally in other models).

The paper is structured as follows: The experimental setup and a description of the parametrization changes considered in this study will be given in section 2. This is followed by the results section which starts with a discussion of systematic errors and their changes for precipitation, convectively-coupled equatorial waves and the extratropical circulation including extratropical cyclones and blocking. In this first part the focus will be on long seasonal integrations. In the second part of the results section, an attempt will be made to better understand the changes due to major modifications to the convection and radiation scheme. To this end the transient response will be studied over a wide range of time scales (from hours to months.) Finally, the discussion is contained in section 4.

Table 1: Main characteristics of the ECMWF model versions used in this study.

Version	Introduced	Modifications
29R2	2005/06/28	Modification to convection scheme
30R1	2006/02/01	Increased vertical resolution (L60 to L91)
31R1	2006/09/12	Revised cloud scheme (ice supersaturation + numerics); implicit computation of convective transports; introduction of turbulent orographic form drag (TOFD) scheme; revised parameterization of sub-grid scale orographic drag
32R1	not operational	New short-wave radiation scheme; introduction of McICA cloud radiation interaction MODIS land surface albedo; retuned ice particle size; retuning of GWD (increase by a factor of two)
32R2	2007/06/05	Minor changes to the forecast model
32R3	2007/11/06	New formulation of convective entrainment and relaxation time scale; reduced vertical diffusion in the free atmosphere; modification to GWD scheme at the top of the model; new soil hydrology scheme
33R1	2008/06/03	Slightly increased vertical diffusion; increased orographic form drag; retuned entrainment in the convection scheme bugfix scaling of freezing term in convection scheme changes to surface model

2 Methods

2.1 Experimental design

2.1.1 Seasonal forecasts

The realism of the ECMWF model climate is assessed using 13 month long integrations with model versions employed operationally at ECMWF since June 2005. The model versions along with their key-changes are summarized in Table 1; a more detailed description of the changes will be given in the following section.

All integrations were carried out using observed daily sea surface temperature (SST) and sea ice fields as lower boundary conditions. Simulations were started on 1 November of each of the years 1962–2005. Results for the standard meteorological seasons (DJF, MAM, JJA and SON) were analyzed. In this study, however, the focus will be on boreal winter. As shown in Jung (2005), 30 days of integration (i.e. the spin-up in November) during boreal winter is enough for systematic atmospheric circulation errors over the Northern Hemisphere to have reached their asymptotic seasonal mean values. All integrations were carried out employing a horizontal resolution of T_L159 (about 1.1°). Integrations with version 29R2 were carried out using 60 levels in the vertical. For model version 30R1 and more recent versions 91 level were used in the vertical.

Additional sensitivity experiments were carried out based on model version 33R1 for winters of the period 1990–2005 in order to better understand the impact that the most recent model changes in radiation, convection, vertical diffusion, soil hydrology and turbulent orographic form drag (see Table 1 and below for more details about those changes) had on the ECMWF model climate. No attempt was made to retune the individual schemes

when implemented in version 33R1.

2.1.2 *Monthly forecasts*

A set of monthly forecasts was carried out in order to study transient aspects of systematic model error and their sensitivity to model formulation using ECMWF model version 33R1 at T_L159 with 91 levels in the vertical. As for the seasonal integrations observed daily SST and sea ice fields were prescribed as lower boundary conditions. Initial conditions were taken from the ERA-Interim reanalysis (Simmons et al. 2007). Monthly forecasts were started on the 15th of November, December, January and February for each of the winters 1989/90–2007/08 (a total of 76 forecasts). Three additional sensitivity experiments were carried out based on model version 33R1, one reverting to the previous convection scheme in isolation, one similarly reverting to the previous radiation scheme, and the third experiment combining both of these changes.

2.2 **Statistical significance**

Statistical significance testing has been used extensively in this study. For reasons of legibility, however, results from statistical significance tests have not been incorporated in most of the figures. In the following all differences between models and observations and different model configurations are statistically significant at the 95% level unless mentioned otherwise.

2.3 **Description of recent parametrization changes**

In the following a more detailed description of key-model changes listed in Table 1 will be given.

2.3.1 *Convection scheme*

A major revision to the convection scheme has been implemented in November 2007 (version 32R3). The changes introduced include a convective entrainment rate that is sensitive to environmental moisture, a deep convection closure where the convective available potential energy is relaxed towards a neutral state using a spatially-varying relaxation time-scale, and a fully implicit numerical formulation. The most important consequence of these changes is that convection and the large-scale dynamics are no longer explicitly coupled through a mass entrainment that is proportional to large-scale moisture convergence. A more detailed description of the changes to the convection scheme along with their impacts on some aspects of the ECMWF model climate are given in Bechtold et al. (2008).

In June 2008 (version 33R1) a constant background entrainment has been added to the relative humidity-dependent entrainment rate in order to reverse the slight degradation in upper-tropospheric tropical winds introduced in version 32R3.

2.3.2 *Cloud scheme*

In September 2006 (version 31R1) a number of changes to the cloud scheme physics and numerics were implemented. The numerical changes were made necessary by the earlier increase in vertical resolution from 60 to 91 levels in version 30R1. This revealed a significant vertical resolution sensitivity of the model climate at

high resolutions, due to a combination of the ice microphysical assumptions and the previous cloud scheme numerical solution methodology (see Tompkins 2008 for details).

The numerical solver for the prognostic cloud water equation was therefore changed to use a forward-in-time upstream implicit solution. In conjunction with this, the previous cloud ice microphysical assumption, that ice settling into sub-cloud clear air is converted into snow, was updated. Instead, from version 31R1, ice settling into sub-saturated cloud free air would undergo sublimation, while the conversion of ice to snow was handled by an explicit autoconversion parametrization. This used the parametric form of Sundqvist et al. (1989) that already represented warm rain processes, with Lin et al. (1983) rate constants that were adjusted for use in a large-scale rather than cloud resolving model, and also to reduce adverse effects on the climate of the model while improving medium-range forecast skill.

At the same time, the opportunity was taken to reject the model assumption that no supersaturation can exist, in favour of a new cloud parametrization that permits supersaturation in clear sky part of gridboxes at cold temperatures below 235K at which homogeneous nucleation occurs. Once ice nucleation has occurred, especially by homogeneous nucleation processes which produce high ice number concentrations with respect to heterogeneous nucleation (Demott et al. 2003), the supersaturation in clear sky is the most important to represent. This is because the rapid growth of ice crystals by deposition reduces the in-cloud supersaturation back towards negligible levels within a typical GCM timestep in all dynamical circumstances bar the strongest of updraughts (Lohmann and Kaercher 2002, Gierens 2003). Details of these complications and the physics of the new scheme itself are given in (Tompkins et al. 2007). In this work, the impact of allowing supersaturation is shown to be that expected; an increase in upper troposphere humidity at the expense of the occurrence and opacity of cirrus ice clouds. Tompkins et al. (2007) also illustrates the improvement of the model with respect to ground-based observations of permanent contrails (a proxy for the existence of a supersaturated air mass) as well as in situ aircraft and remote satellite observations of upper tropospheric humidity and supersaturation.

2.3.3 Orography

The Turbulent Orographic Form Drag (TOFD) parametrization of Beljaars et al. (2004b) was introduced in the ECMWF model in September 2006 (model version 31R1) to represent drag on the flow due to sub-grid scale orography (SSO) with horizontal scales below 5000 m. TOFD is an alternative to the previously used “effective roughness length” concept. The scheme is controlled by the standard deviation of subgrid orography in the scale range of 2 to 20 km, derived from a 1 km orographic data set. The desired spectral range of sub-grid scale orography with scales smaller than 5000 m is obtained by assuming a universal power spectrum. In June 2008 (version 33R1) a constant of proportionality in the TOFD parametrization (see Eqn. (15) in Beljaars et al. (2004b)), has been increased from 12 to 27. This is equivalent to an increase of the standard deviation of the SSO by a factor 1.5.

Version 31R1 included a ‘cutoff’ or ‘effective’ mountain height in the computation of gravity wave drag from the SSO scheme. The more physically realistic cutoff mountain height resulted in a decrease in gravity wave drag (GWD), reducing the excessive deceleration of flow over the Himalayas and Rocky Mountains (Orr, 2007). However, climate runs showed an increase in the positive zonal wind bias over winter northern hemisphere mid-latitudes, suggesting that the reduction in GWD had been excessive. This problem was solved in version 32R1 by doubling the ‘cutoff’ mountain height and thereby increasing the amplitude of the gravity waves ‘generated’ by the SSO scheme by a factor of two.

TOFD, SSO gravity wave drag and low-level blocking momentum tendencies can be significant over orography, resulting in large increments when the model time step is long. Moreover, to some extent the processes are coupled, leading to a time step sensitivity if each of the relative parameterization schemes evaluates its

tendencies independently (Beljaars et al. 2004a). However, some degree of dependency (and a corresponding reduction in time step sensitivity) was introduced in version 31R1 by solving the relevant momentum tendency coefficients in a joint implicit calculation (Orr 2007).

2.3.4 Vertical diffusion

Turbulent diffusion in the stable boundary layer and in the free troposphere is larger than that expected from local Monin-Obukhov (MO) similarity theory in many models, including the ECMWF model, which employs the Louis, Tiedtke and Geleyn (1982) scheme (LTG hereafter). In order to increase the realism of the ECMWF model, the diffusion coefficients were reduced to values consistent with MO theory above the surface layer in November 2007 (version 32R3, see Bechtold et al. 2008 for details). This change led to stronger shears and inversions, more stratocumulus (10–30% locally), colder ($-0.3K$) and moister ($0.1gkg^{-1}$) near-surface atmosphere over land (based on annual mean observational data), stronger ageostrophic winds and larger baroclinic growth rates in the extratropical storm tracks. These changes are all improvements over previous model versions.

The larger baroclinic growth rates interestingly improved the short-term accuracy of the model (day 1–3), yet led to excessive activity and a worsening of objective scores in the medium-range up to 10 days. Unresolved shear instability was identified as a missing source of turbulence in the model. An investigation of power spectra of vertical shear in the ECMWF model simulations at T_L95 to T_L2047 indicated too little shear near grid truncation scales. This shear deficiency, which amounts to about 20%, peaks at around 900hPa. Parameterising this shear component in the diffusion coefficient explains about half of the LTG diffusion increase over MO theory. Additionally, it was noted that the TOFD parameterization is working sub-optimally when coupled with MO diffusion coefficients. With an adjustment of the TOFD coefficients in model version 33R1 a significant performance improvements could be achieved.

In summary, the LTG broadly enhanced diffusion formulation was replaced with MO theory in version 32R3. An additional parametrization of the turbulent source from unresolved shear and orography was added in model version 33R1. The combined new formulation still produces considerably less stable layer turbulent transport than the LTG formulation with better model performance.

2.3.5 Radiation

A new package of radiation transfer parametrisations was introduced in the ECMWF model with version 32R1. It includes the short-wave part of the Rapid Radiation Transfer Model (RRTM: Iacono et al. 2008) (complementing the long-wave part of RRTM (Mlawer et al. 1997) introduced into the ECMWF model in June 2000), the Monte-Carlo Independent Column Approximation (McICA: Barker et al. 2002, Pincus et al. 2003), revised ice cloud radiative properties, and a more extensive use of a reduced radiation grid. The impact of this new radiation package on various configurations of the ECMWF forecasting system is discussed in Morcrette et al. (2008a,b).

2.3.6 Soil hydrology

A revised soil hydrology has been introduced in June 2008 (version 33R1) for the Tiled ECMWF Scheme for Surface Exchanges over Land (HTESSEL: Viterbo and Beljaars 1995, Viterbo et al. 1999, van den Hurk et al. 2000, Balsamo et al. 2008). The revision addressed two main short-comings of the land surface scheme: the absence of surface runoff and a global uniform soil texture. A new dataset for soil type based on the

Food and Agriculture Organization (FAO) was included, and hydrological classes (up to six) were assigned to each grid cell. A revised infiltration scheme with sub-grid surface runoff description was also introduced and evaluated. In point comparisons with field site experiments these modifications show a shift in the soil moisture range to give better agreement with observations. The soil physiographic parameters (wilting point and field capacity) associated to each soil texture produced a larger soil water holding capacity. In drylands the shift of the soil moisture range gave slightly better evaporation. The inter-annual variability of root-zone soil moisture showed improvements with a satisfactory match to a 8-year continuous dataset. Quantitative evaluation of the land surface runoff at monthly time-scales shows a net improvement of runoff timing in relevant catchments, when evaluated in a set of regional stand-alone experiments (see Balsamo et al. 2008 for details). Atmospheric coupled hindcasts revealed a small positive impact on the model climate. A reduction of data assimilation increments at the surface was obtained in the ECMWF model for the soil moisture field.

3 Results

3.1 Model climate

3.1.1 Precipitation

The observed mean precipitation climatology during boreal winter from the Global Precipitation Climatology Project (Adler et al. 2003) is shown in Figure 1a. Largest values are found in the tropics, particularly over central South America, Africa and the Maritime Continent. In the Northern Hemisphere extratropics the largest mean precipitation is found in North Atlantic and North Pacific storm tracks.

Model versions 29R2, 30R1 and 31R1 show very similar systematic precipitation errors, both in the tropics and extratropics: In the tropics, precipitation is generally too weak (strong) over the continents (oceans). Positive precipitation biases are particularly problematic in the tropical Atlantic, the southern parts of the Caribbean (in relative terms), the Indian ocean, and just north off the equator in the tropical Pacific. Positive precipitation biases in the eastern North Atlantic are indicative of an underestimation of Euro-Atlantic blocking events and a too weak storm track in higher latitudes (see below, for more details). It is worth pointing out that the above-mentioned precipitation biases have been a feature of the ECMWF model for many years (e.g., Brankovic et al. 2002, Jung and Tompkins, 2003).

Changes in version 32R1 (see Table 1) led to a substantial increase of precipitation over tropical continents which, over the Southern Hemisphere, extends well into subtropical regions. For central South America and parts of the Maritime Continent this increase is beneficial in reducing the “dry bias” of earlier model versions. The precipitation increase in model version 32R1 over central and southern parts of Africa seems to be detrimental.

The largest change of systematic precipitation errors occurred with the introduction of version 32R3. Mean precipitation changes were mostly beneficial in the sense that they led to reduced systematic precipitation errors. This is particularly true in the central and eastern tropical Pacific, in the Caribbean and over central South America. In other areas such as the Andes and near Papua New Guinea, version 32R3 led to increased precipitation biases. Finally, it is worth pointing out that even for the most recent model version considered in this study (33R1), there are still substantial systematic errors in simulating mean precipitation including regions such as the tropical Indian ocean and the western tropical Pacific.

Figure 2 shows systematic precipitation errors for sensitivity experiments with model version 33R1 in which specific parametrization schemes have been replaced by their predecessors. Evidently, the introduction of the

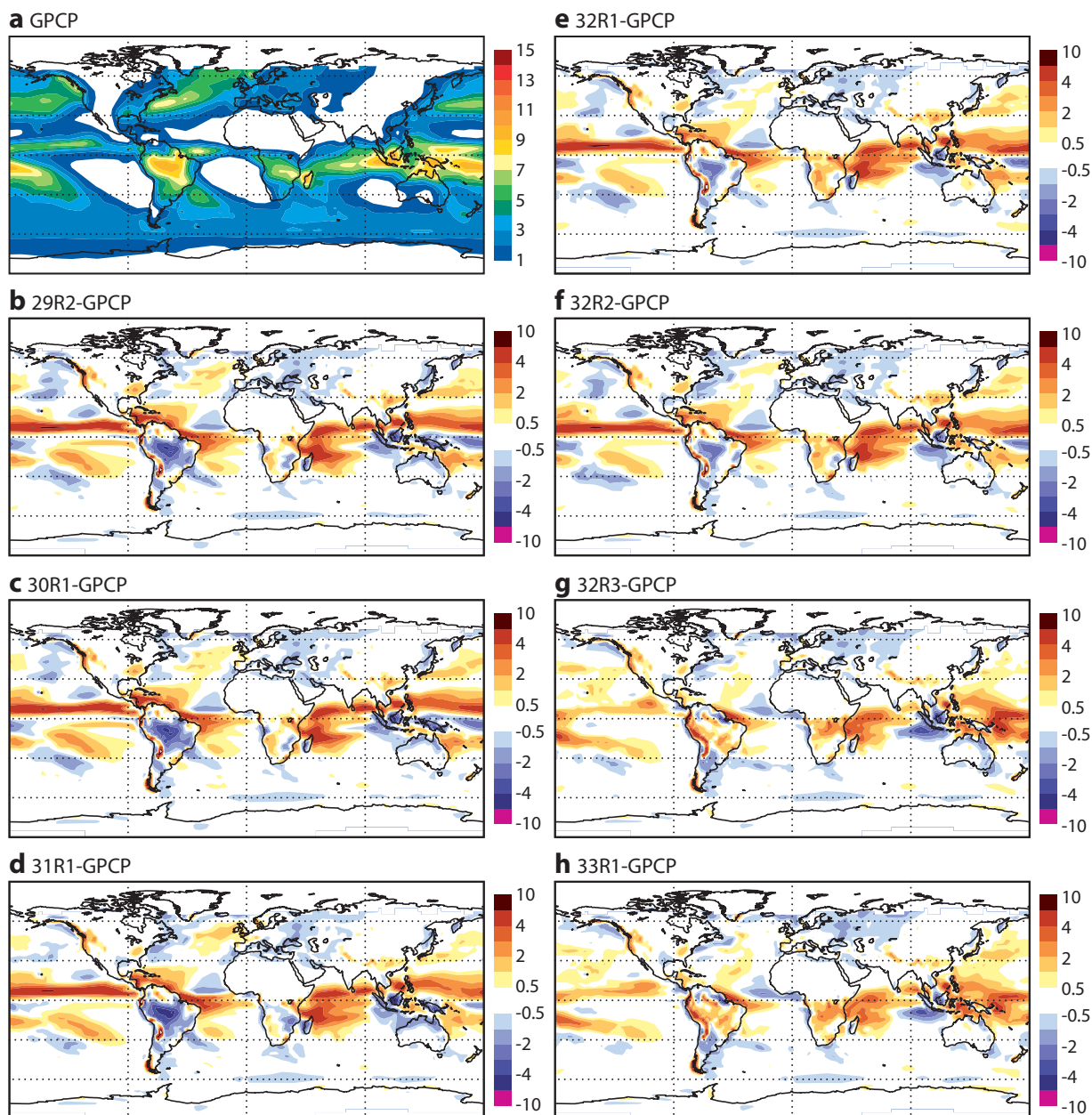


Figure 1: Observed mean precipitation (mm day^{-1}) from GPCP for winters (December–February) of the period 1979–2001 (upper left panel) along with systematic precipitation errors for various versions of the ECMWF model: (b) 29R2, (c), 30R1, (d) 31R1, (e) 32R1, (f) 32R2, (g) 32R3 and (h) 33R1. Model climatologies have been computed using data from 1962–2005.

new radiation scheme in version 32R1 was responsible for reduced dry biases over the tropical continents. The bulk of the improvements in tropical mean precipitation, seen with the introduction of version 32R3, on the other hand, can be explained by the new convection scheme. The influence of changes in vertical diffusion, TOFD and the soil hydrology scheme on mean precipitation fields turns out to be relatively small (Figure 2).

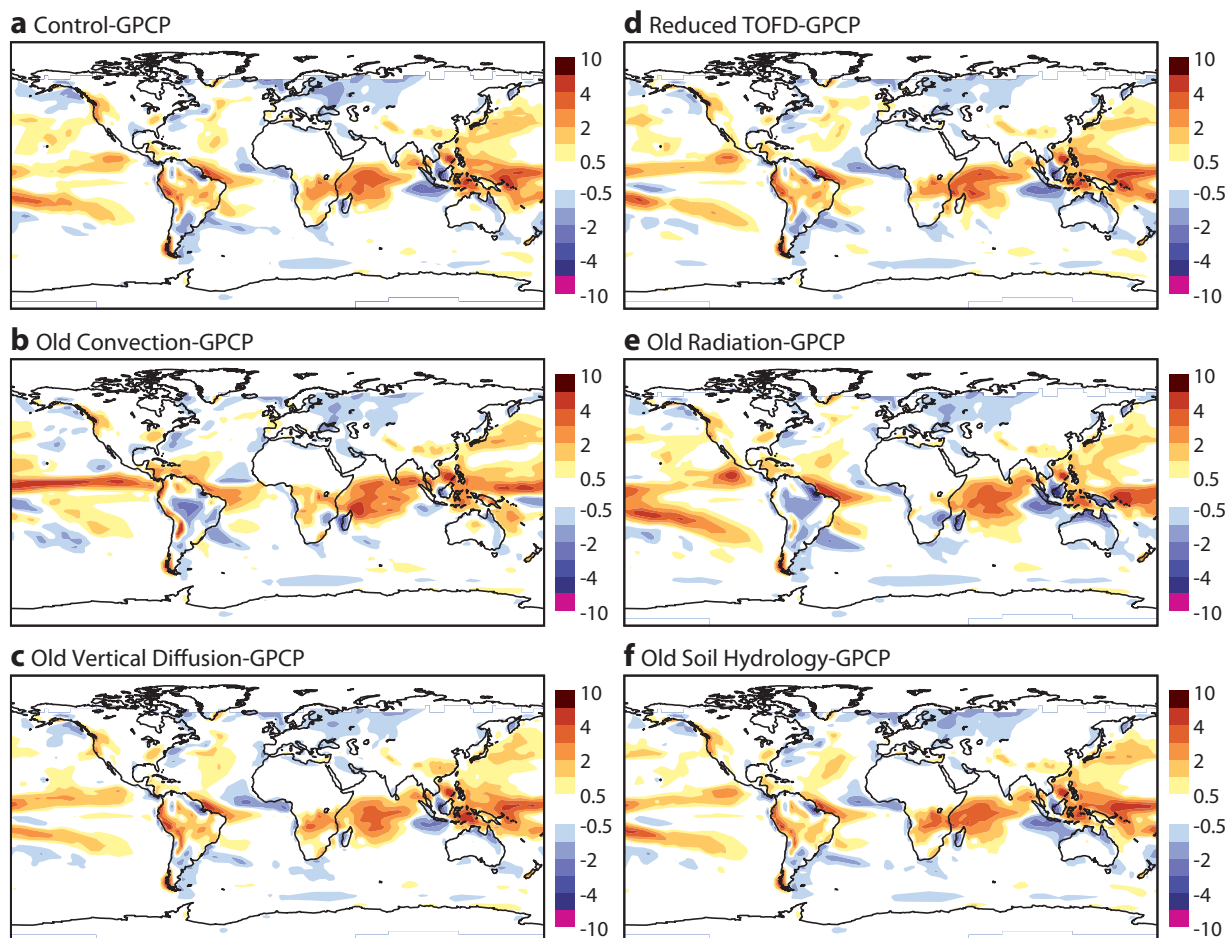


Figure 2: Systematic precipitation error (mm day^{-1}) during wintertime (December–February) for version (a) 33R1, (b) 33R1 with convection from 32R2, (c) 33R1 with vertical diffusion from 32R2, (d) 33R1 with reduced TOFD from 32R3, (e) 33R1 with radiation scheme from 31R1 and (f) 33R1 with soil hydrology scheme 32R2. Results are based on differences of mean fields between the model (1990–2005) and observational estimates from GPCP (1979–2001).

3.1.2 Extratropical circulation

Figure 3 shows how recent model changes have influenced mean atmospheric circulation errors in terms of Northern Hemisphere 500 hPa geopotential height fields (Z500, hereafter) during boreal winter. Very similar errors—reflecting too strong a zonal flow—are found for model versions 29R2 to 32R2. In fact, for earlier model versions a very similar systematic error structure was found for Z500 (e.g., Brankovic et al. 2002, Jung 2005). With the introduction of model version 32R3 in November 2007, however, systematic Z500 error in the North Pacific/North America region reduced substantially. The same is true for the North Atlantic region (Figure 3), where the circulation was too cyclonic from model version 29R2 to 32R2. In version 31R1 this error was further enhanced due to an excessively strong stratospheric polar vortex in the 91 level version of the model (not shown) which was a result of a too weak drag exerted by the SSO gravity wave parametrization in the stratosphere (Orr 2007).

Additional sensitivity experiments for winters of the period 1990–2005 based on model version 33R1 (not shown) shed some light on the role of the various parametrization changes. The introduction of the new convection scheme, introduced in version 32R3, reduced systematic Z500 errors over the North Pacific, North America. In the Euro-Atlantic region, both the introduction of the new convection scheme and the increase of

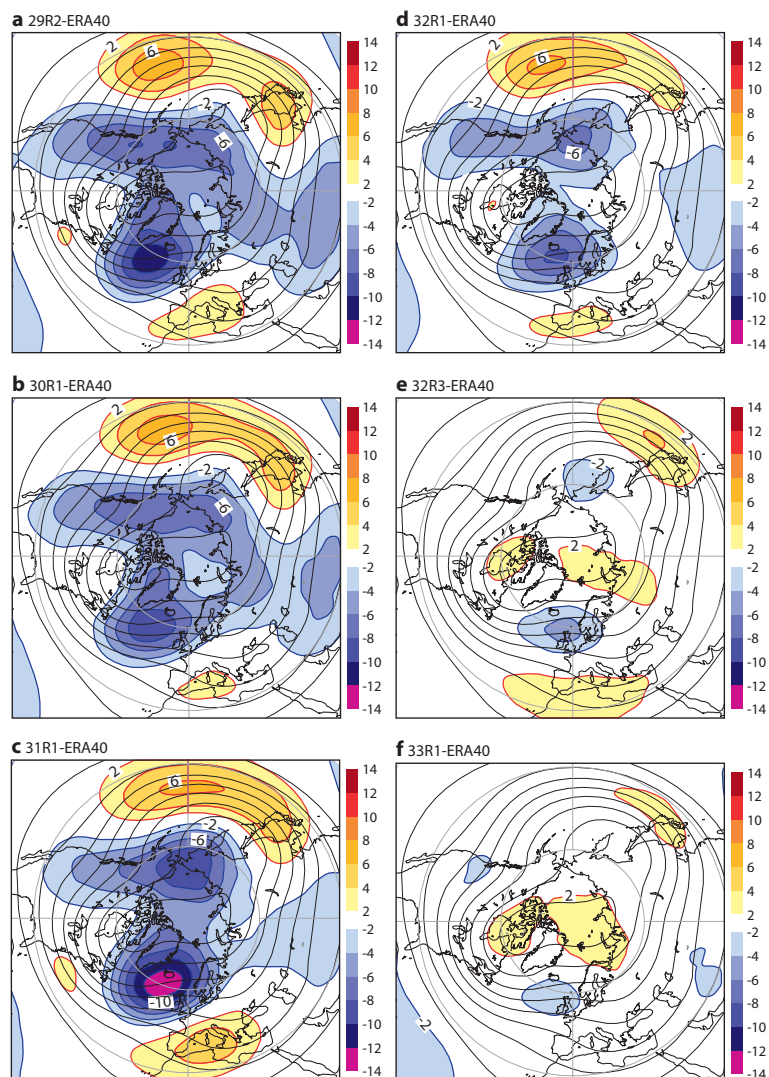


Figure 3: Mean systematic errors of 500 hPa geopotential height fields (shading in dam) for winters (December–February) of the period 1962–2005 and various versions of the ECMWF model: (a) 29R2, (b) 30R1, (c) 31R1, (d) 32R1, (e) 32R3 and (f) 33R1. Also shown are mean fields (contours) obtained from a combination of ERA-40 (1962–2001) and operational ECMWF analysis data (2002–2005). Mean systematic errors significant at the 95% confidence level are hatched. Notice that negative values are contoured (as well as shaded).

TOFD led to a reduction of the westerly wind bias.

3.1.3 Blocking

The capability of models to capture the observed frequency of blocking events is crucial, given the importance of blocking for local weather conditions. This is particularly true for Europe where, during wintertime, blocking events lead to an interruption of the predominantly mild southwesterly winds. It is well-known that many climate models underpredict the observed frequency of occurrence of blocking, particularly in the Euro-Atlantic region (e.g., D’Andrea et al. 1998, Boyle 2006). The same is certainly true for earlier versions of the ECMWF model (e.g., Jung 2005).

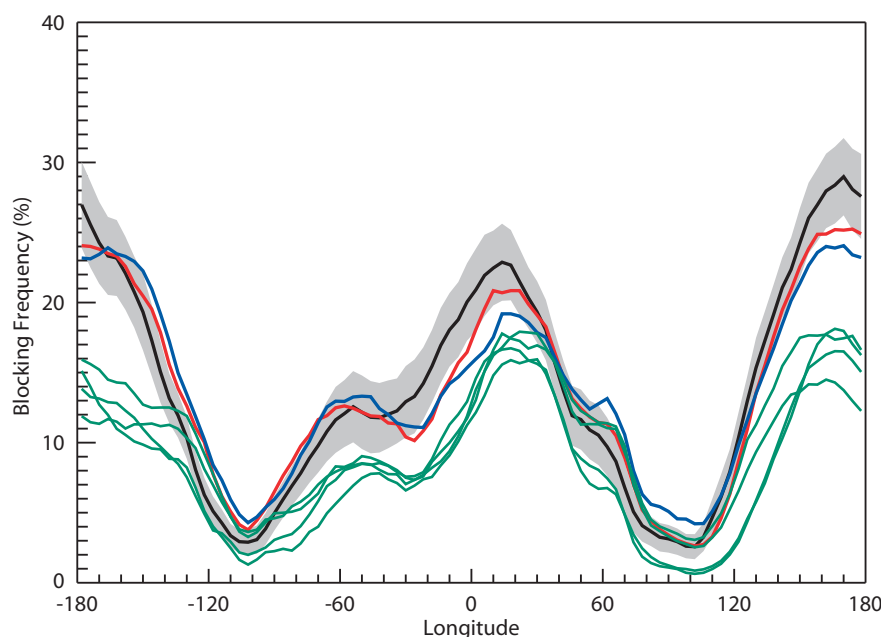


Figure 4: Frequency of occurrence of wintertime Northern Hemisphere blocking events (December–February) for the period 1962–2005: ERA-40 (black), version 33R1 (red), version 32R3 (blue) and versions 29R2–32R2 (green). Blocking frequencies have been determined using the methodology by Tibaldi and Molteni (1990). Also shown are 95% confidence intervals for ERA-40 data (grey shading).

The observed and simulated frequency of occurrence of Northern Hemisphere blocking using model versions 29R2 to 33R1 are shown in Figure 4 for winters of the period 1962–2005. Here, blocking frequencies were computed using the method introduced by Tibaldi and Molteni (1990). The observations show two well-known maxima in the North Pacific and Euro-Atlantic region. In the North Pacific region simulated blocking frequencies were substantially underestimated until the introduction of model version 32R3 (blue and red curves). The same is true for the Euro-Atlantic region. It is highlighted that in the Euro-Atlantic region, for the first time, it is possible to obtain realistic blocking frequencies in climate simulations (at T_L159) with version 32R3 and 33R1. In the North Pacific region, on the other hand, similar improvements have been previously achieved by the introduction of a more realistic aerosol climatology in October 2003 (Rodwell and Jung 2008) (the error re-appeared in the following model version) and by implementing a stochastic parametrization of subgrid-scale physical processes (Jung et al 2005). The fact that differences in the blocking frequencies between model version 29R2 to 32R2 are much smaller than the impact that the introduction of version 32R3/33R1 had highlights the significance of the changes to the convection scheme and the increased TOFD.

The additional sensitivity experiments with version 33R1 reveal that improved blocking frequencies in the *North Pacific* with the introduction of version 32R3 can primarily be explained by changes to the convection scheme (not shown). For *Euro-Atlantic* blocking events, on the other hand, both the new convection scheme and larger TOFD increase the frequency of occurrence of blocking. The impact of the changes to the vertical diffusion and radiation scheme are of secondary importance; and the impact of the soil hydrology scheme on the frequency of occurrence of Euro-Atlantic blocking events is negligible.

3.1.4 Synoptic activity

Previous studies have revealed that older versions of the ECMWF model tend to underestimate the level of synoptic activity in high latitudes of the Northern Hemisphere (Jung 2005), especially at relatively low hor-

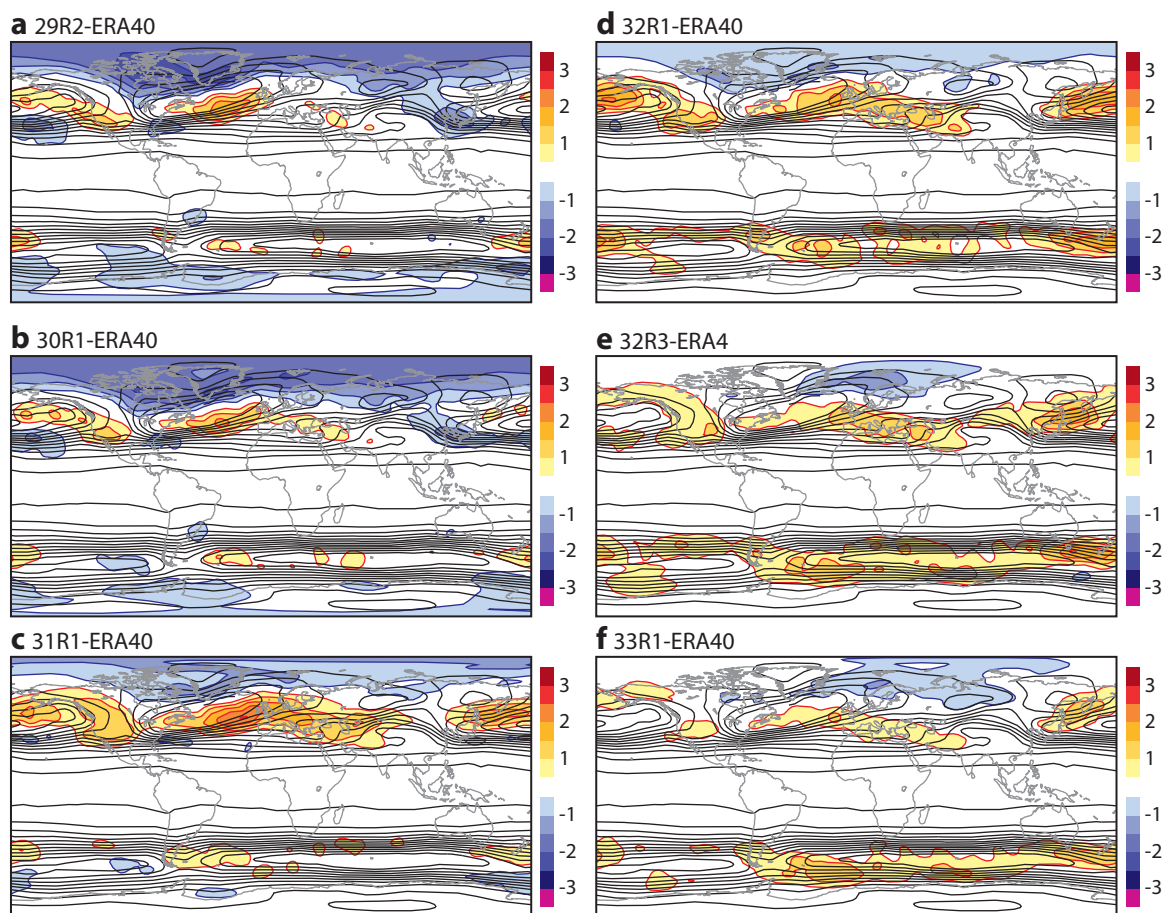


Figure 5: As in Fig. 3, but for synoptic activity of 500 hPa geopotential height fields (shading in mday^{-1}). Notice that negative values are contoured (as well as shaded).

horizontal resolutions (Jung et al. 2006) such as the one employed in this study (i.e., T_L159). Figure 5 shows systematic errors in synoptic activity of daily Z500 fields for model versions 29R2 to 33R1. Here, “synoptic activity” is defined as the standard deviation of highpass-filtered Z500 fields. A tendency filter was employed for highpass-filtering (see Jung 2005 for details). Two major improvements stand out. Firstly, the introduction of version 31R1 led to higher, and more realistic levels of synoptic activity in the high-latitudes of the Northern Hemisphere. One possible explanation for this improvement is the revision to the cloud scheme (in particular the more realistic treatment of ice supersaturation). An additional sensitivity experiment with version 30R1, in which the new cloud scheme of version 31R1 is used, confirms this conjecture (Figure 6). Secondly, there was a distinct improvement over the Northern Hemisphere with the introduction of version 32R3 (Figure 5), particularly in the North Pacific region. Additional experiments reveal that the improvement over the Northern Hemisphere can largely be explained by changes to the convection scheme and increased TOFD (not shown). This is consistent with the results obtained for the large-scale atmospheric circulation (see above). The changes in vertical diffusion (in version 32R3) led to a significant and beneficial increase in the level of synoptic activity in the North Atlantic storm track and in the Nordic Seas.

In the Southern Hemisphere the level of synoptic Z500 activity seems to have deteriorated slightly (implying that the model is overactive) with the introduction of version 32R1 (Figure 5). In fact, the increased level of synoptic activity in the Southern Hemisphere storm tracks in version 32R1 is a feature of all seasons (not shown). The results are based on the period 1962–2005, which includes the pre-satellite era for which only

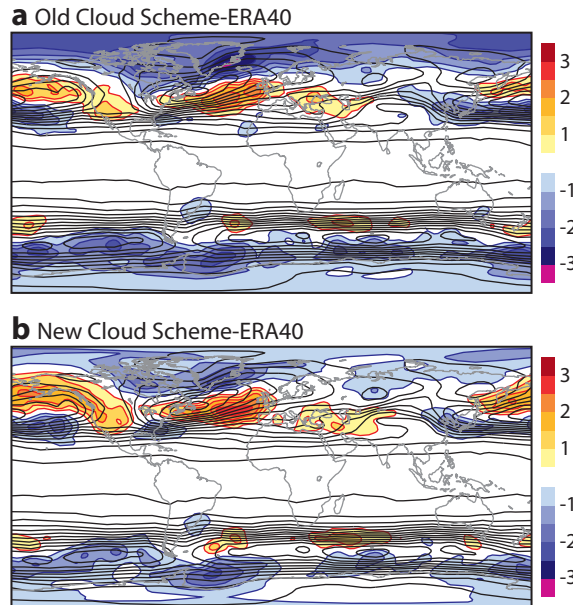


Figure 6: As in Fig. 5, but for the period 1990–2005: (a) control integration with version 30R1 and (b) 30R1 with new cloud scheme from version 31R1. Notice that negative values are contoured (as well as shaded).

relatively few observations were available to constrain the reanalysis (i.e. model particularities influence the reanalysis). The same diagnostics computed for the satellite era only (1980–2005) show that the increase in synoptic activity in the Southern Hemisphere with the introduction of version 32R1 was actually beneficial (not shown). For the Northern Hemisphere the results are much less sensitive to the choice of the period (pre satellite vs satellite era), which can be explained by the availability of a much better conventional observation system.

3.1.5 Convectively coupled tropical waves

Previous studies show that current state-of-the-art general circulation models display a wide range of skill in simulating convectively coupled tropical waves (e.g., Lin et al. 2006). Wavenumber-frequency spectral analysis of outgoing longwave radiation (OLR) anomalies is the most commonly used way to diagnose convectively coupled tropical waves (Wheeler and Kiladis 1999). Observational data suggest that relatively more power is located in the eastward propagating Kelvin wave part, including the Madden-Julian oscillation (MJO), than in the westward propagating Rossby wave part. For the ECMWF model the opposite was true for model versions prior to 32R3; with the introduction of 32R3, however, the wavenumber-frequency characteristic of tropical OLR anomalies became much more realistic (not shown, see Bechtold et al. 2008 for further details).

The changes described in Bechtold et al. (2008) are analysed in more detail, with the left panels of Figure 7 showing wavenumber-frequency diagrams for the symmetric component of tropical precipitation anomalies in version 32R2 produced by the cloud (upper panels) and convection scheme (lower panels). Note that the split into “large-scale” and convective rainfall does not necessarily reflect real-world physics, but it is useful for diagnostics purposes (Tompkins and Jung, 2004). In version 32R2, the contributions from the cloud scheme and the convection scheme are comparable in terms of variance. Following a suggestion by Tompkins and Jung (2004), one might explain the change towards increased convectively coupled Kelvin wave activity in model version 32R2 by an increase in the relative contribution of the cloud scheme to the total precipitation variability. The right panels of Figure 7, which depict corresponding diagnostics for version 32R3, shows that

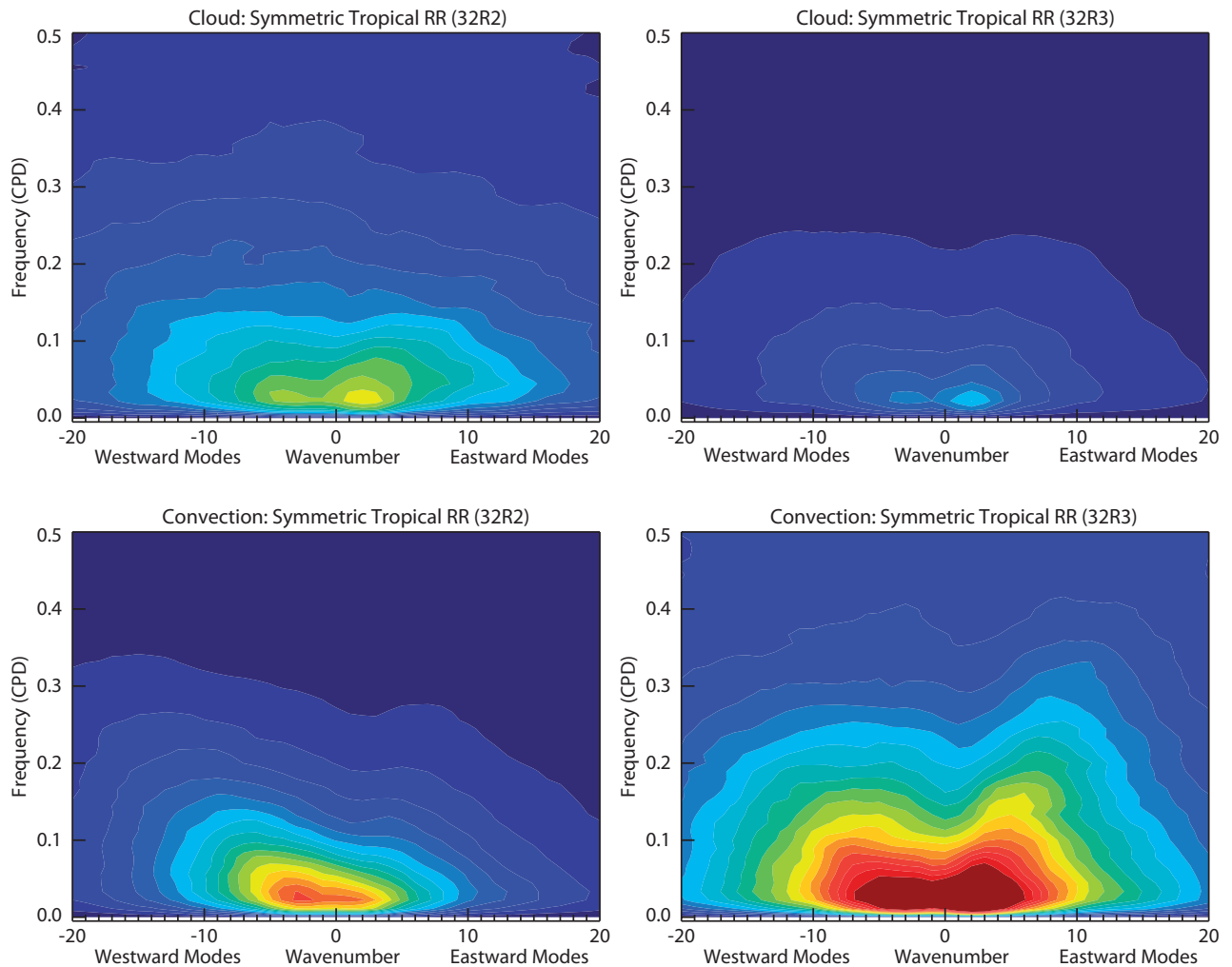


Figure 7: Mean wavenumber-frequency spectra for the symmetric component of precipitation computed by the cloud (upper panels) and convection scheme (lower panels) for model version 32R2 (left) and 32R3 (right). Results are based on winters of the period 1962–2005. The mean annual cycle has been removed prior to the computation of the wavenumber-frequency spectra. The same contour interval is used in all four panels.

this is *not* the case. In fact, in version 32R3 the convective precipitation scheme has a much larger contribution to total precipitation anomalies than in previous versions. Moreover, the *structure* of the wavenumber-frequency spectrum for convective precipitation has changed in version 32R3; with Kelvin waves playing a much more important role. The reason for these changes, however, is not yet fully understood and is subject of ongoing research.

3.2 Transient adjustment

From the results based on the seasonal integrations discussed so far it is very difficult to understand how exactly changes in model formulation affect the climate of the model, since longer model integration permit the various processes to interact. Furthermore, in long integrations model problems may influence remote regions through wave processes making it difficult to decide whether a certain change is of local or remote origin (e.g. Rodwell and Jung 2008). In the following, an attempt is made to better understand the influence of the changes to the

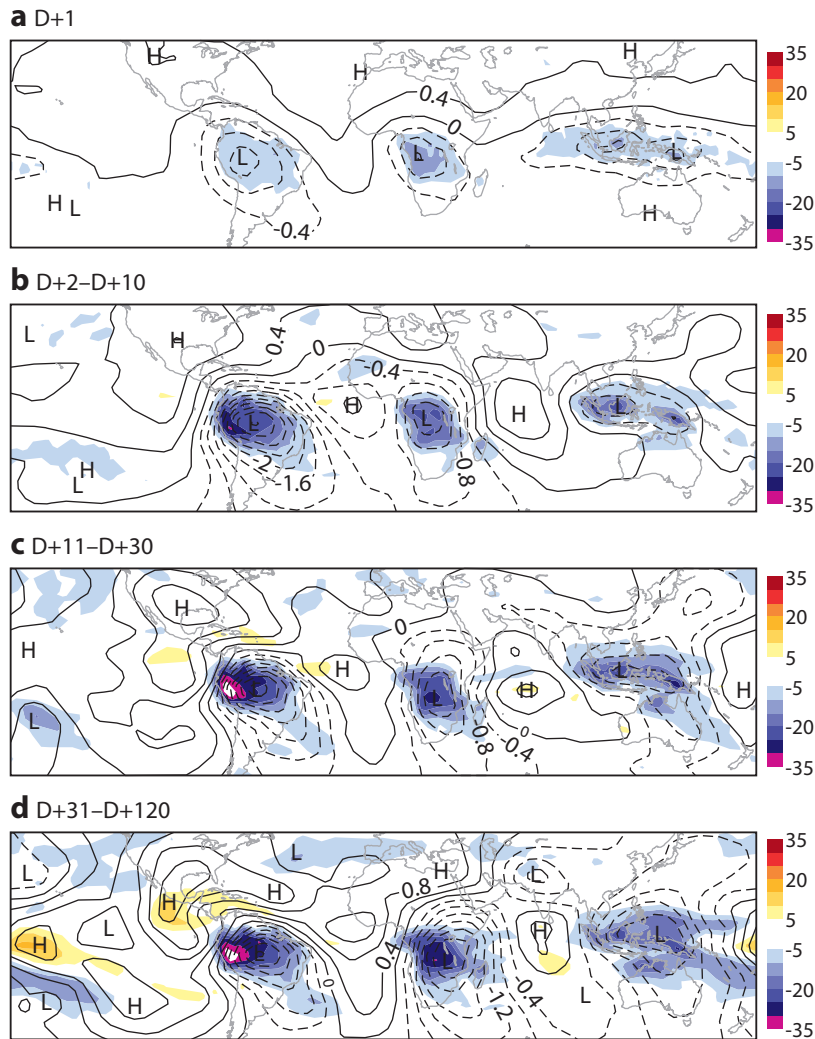


Figure 8: Mean difference in velocity potential at 200 hPa (contour interval is $0.4 \text{ m}^2\text{s}^{-1}$, negative values are dashed) and outgoing long wave radiation (shading in Wm^{-2}) between the experiments with new and old radiation scheme: (a) D+1, (b) D+2–D+10, (c) D+11–D+30 and (d) D+31–D+120. Experiments were carried out with model version 33R1: (a)–(c) monthly forecasts and (d) seasonal forecasts (see Methods for details). Notice that negative values for OLR are contoured (as well as shaded). OLR is defined positive upwards.

radiation and convection scheme. To this end, the transient adjustment of the models from the first day of the integration up to the time at which most of the adjustment has completed (about one month) is considered. Differences from D+1 to D+30 are based on monthly forecasts and those from D+31 to D+120 on seasonal forecasts. It should be noted, therefore, that while both cover the winter season December through March, the different forecast ranges considered here (D+1, D+2–D+10, D+11–D+30 and D+31–D+120) sample slightly different periods.

3.2.1 Influence of radiation scheme

Differences in OLR and the velocity potential at 200 hPa (χ_{200}) between a model run with new and old radiations scheme is shown in Figure 8 for various forecast ranges. Within approximately the first 10 days of the integration the ECMWF model with the new radiation scheme reaches its new equilibrium in the tropics. The

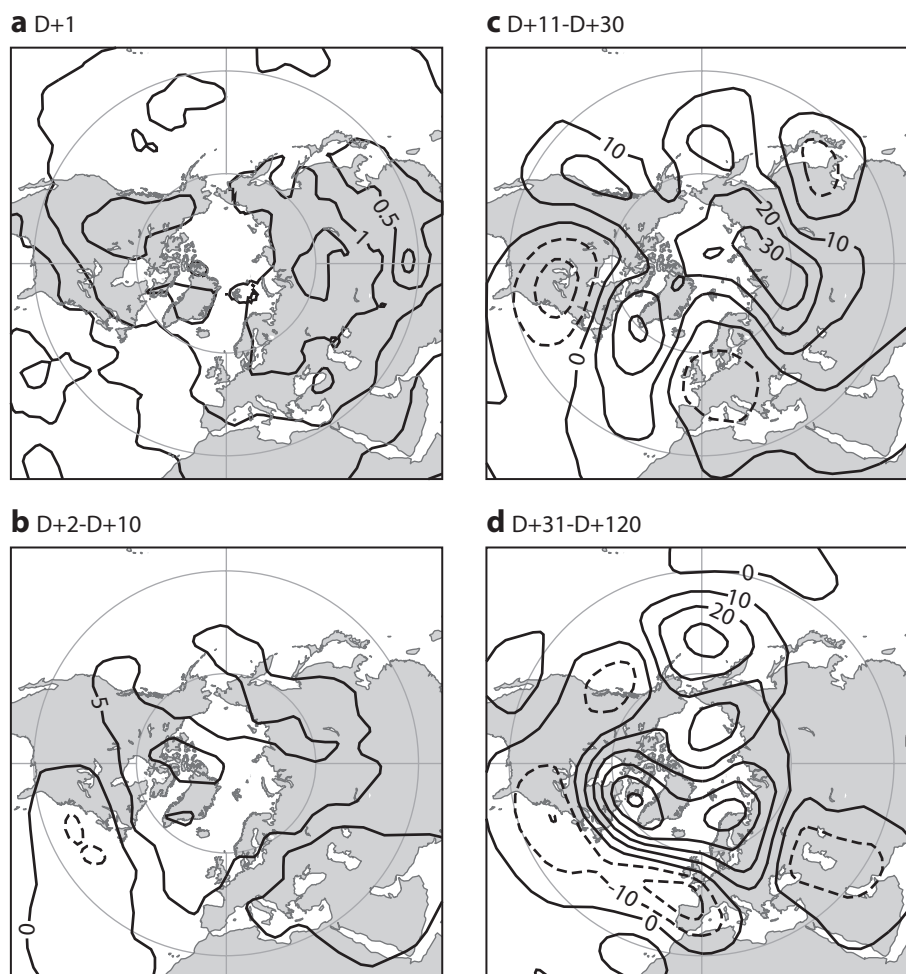


Figure 9: Mean difference in 500 hPa geopotential height (in m) between experiments with the new and old radiation scheme: (a) D+1, (b) D+2–D+10, (c) D+11–D+30 and (d) D+31–D+120. Contour interval is (a) 0.5 m, (b) 5 m and (c)–(d) 10 m. Experiments were carried out with model version 33R1: (a)–(c) monthly forecasts and (d) seasonal forecasts (see Methods for details).

influence of the new radiation scheme is largest over tropical land areas including the Maritime Continent and encompasses increased convective activity (the contribution from the cloud scheme remains unchanged, not shown), reduced OLR and increased upper-tropospheric divergent outflow. The structure of the atmospheric response at D+1 (Fig. 8a), which localizes the primary sensitive regions, suggests that interaction between radiation, the surface and convection are crucial. This is in line with the mechanism put forward by Morcrette et al. (2008a), that is, more solar radiation reaches the surface with the new radiation scheme, which leads to enhanced convection. The increased convective heating is balanced by the large-scale dynamics in form of large-scale ascent. The streamfunction response at 200 hPa (not shown) associated with the diabatic heating anomalies is reminiscent of linear equatorially trapped Kelvin waves (e.g. Hendon 1986).

In the extratropics no mean influence of the new radiation scheme on Z500 is seen during the first 10 days or so into the forecasts (Fig. 9). Beyond D+10, however, a significant mean Z500 response is established. Supported by tropical and subtropical stream function anomalies in the upper troposphere (not shown), the Z500 response shown for the North Atlantic region is consistent with a Rossby wave train emanating from South America. Beyond the first month of the integration the tropical origin of the wave train becomes somewhat less apparent; this could partly be explained by the influence of other remote effects and by eddy-mean flow interactions in

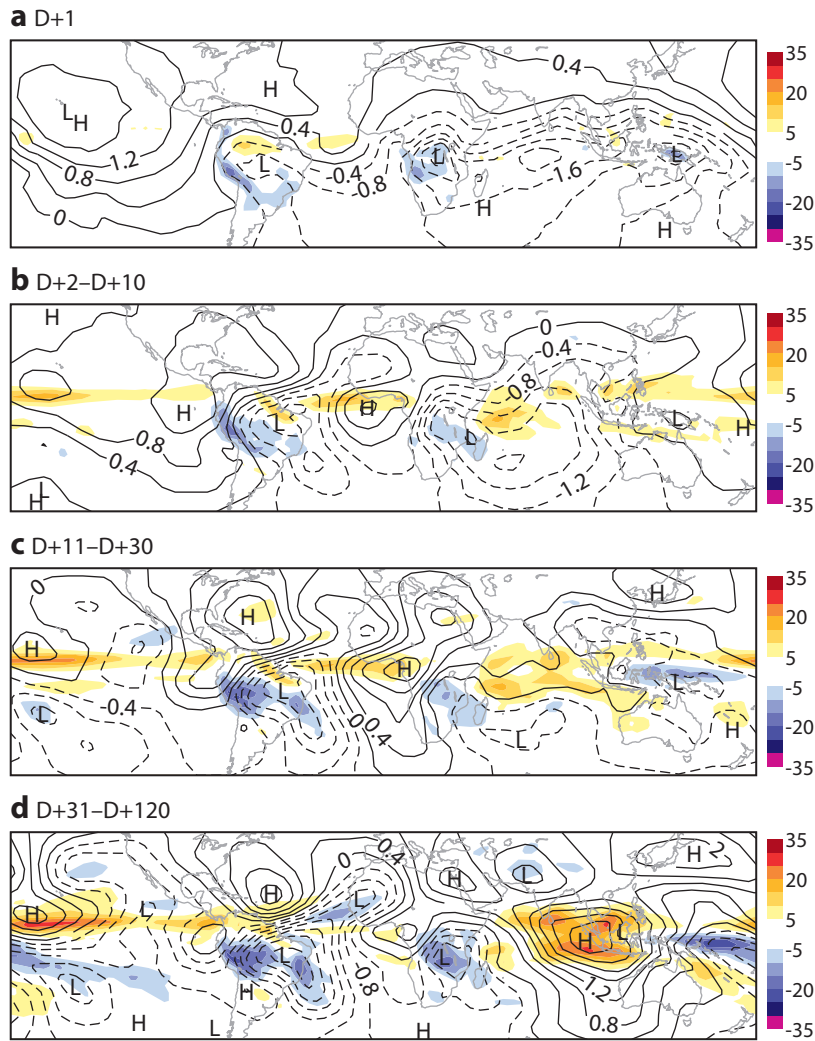


Figure 10: Same as in Fig. 8, but for the difference between the new and old convection scheme.

the North Atlantic storm track.

3.2.2 Influence of convection scheme

The initial response (D+1) in the tropics over land to the introduction of the new convection scheme (Fig. 10a) is similar to that seen with the new radiation scheme (Fig. 8a). This suggests that the mechanism over land is somewhat similar. Over sea, the opposite response can be found, that is, convective activity is reduced and the large-scale circulation responds such that the reduced convective heating is balanced by reduced adiabatic ascent. Throughout the forecast the response to the new convection scheme remains relatively stable, especially over land. However, there also appears to be some modification (e.g. tropical Pacific and Indian ocean) suggesting that non-local processes come into play.

Unlike for the radiation scheme, the introduction of the new convection scheme has an *immediate* (D+1) influence on mean Z500 forecasts in the extratropics (Fig. 11a) suggesting that the convection change did have an influence on extratropical dynamics. On average, D+1 forecasts of Z500 are higher in the North Pacific and

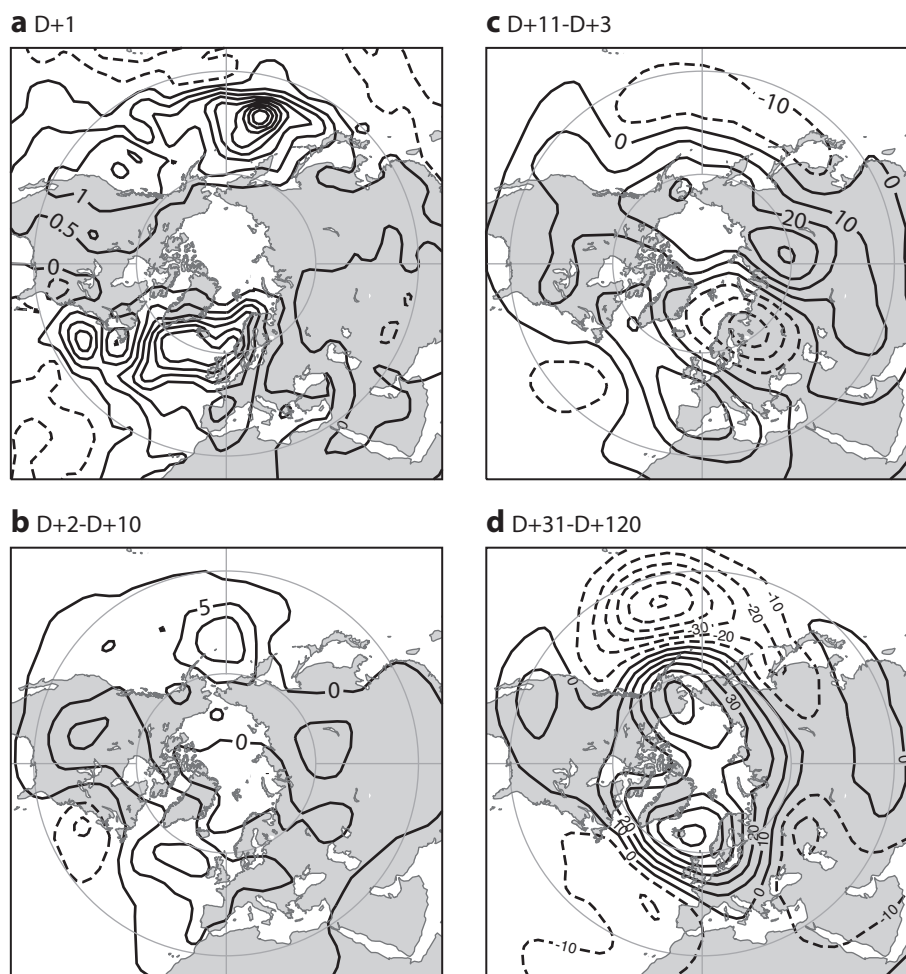


Figure 11: As in Figure 9, but for the difference between new and old convection scheme.

North Atlantic region. Figure 12 reveals that higher (lower) values for Z500 (relative vorticity) with the new convection scheme occur primarily for cyclonic circulation features. The largest changes occur in areas of cold-air outbreaks associated with medium-to-large amplitude Rossby waves, where the more active new convection provides more vertical stabilisation in the convectively unstable cold cyclonic sector through vertical mixing and condensational heating (not shown). The more active convective damping therefore appears to prevent spurious intensification of cold sector cyclonic systems eventually affecting weather further downstream.

Throughout the forecast the mean Z500 response changes somewhat, especially in the North Pacific. As for the radiation scheme, it is plausible that the extratropical response is modified by stationary Rossby wave trains which are triggered by changes in mean tropical diabatic heating (Fig. 10). However, given the direct influence of the changed convection scheme on the intensity of extratropical cyclones, a reduction of the strength of the westerly winds in the North Pacific and North Atlantic on seasonal time scales might be explained by a reduction in large-scale streamfunction forcing by the transient eddies (see, e.g., Hurrell 1995 for details on the transient eddy forcing of the large-scale rotational flow).

Given that the new convection scheme shows a significant influence in the extratropics early on in the forecasts it is worth asking whether the introduction of the new convection has been beneficial in terms of short-range and medium-range predictive skill. The difference in mean absolute error of D+1 to D+4 Z500 forecasts between the model with new and old convection scheme is shown in Figure 13. The introduction of the new

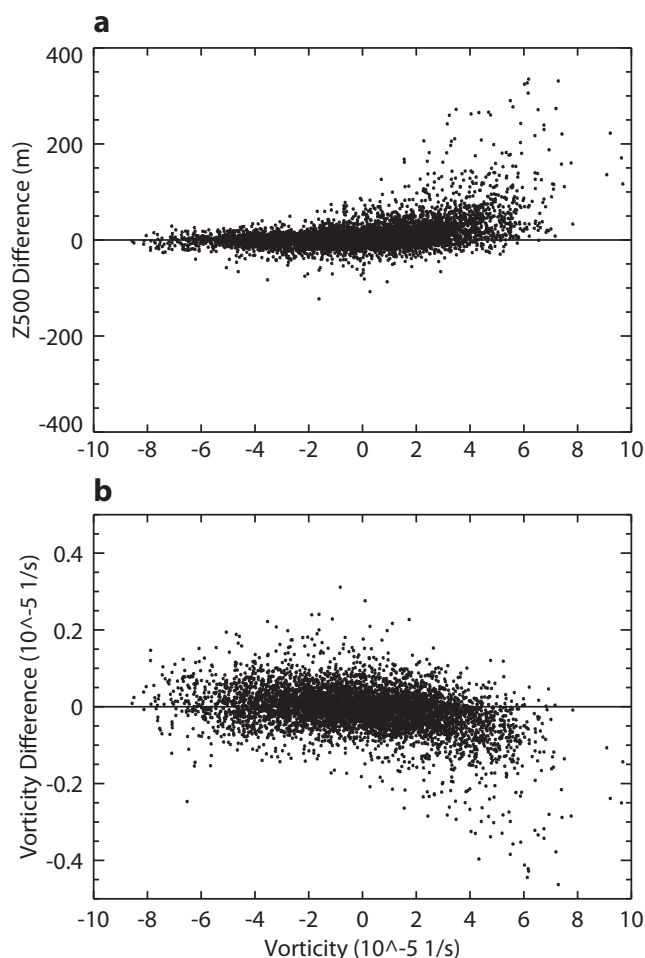


Figure 12: Difference in (a) Z500 (in m) and (b) relative vorticity (10^{-5} s^{-1}) between D+1 forecasts with new and old convection scheme as a function of D+1 relative vorticity with old convection scheme. Results are shown for all grid points (regular $5^\circ \times 5^\circ$ latitude-longitude grid) in the Euro-Atlantic region ($40\text{--}65^\circ \text{N}$ and $50^\circ \text{W}\text{--}10^\circ \text{E}$). Relative vorticity (Z500) was spectrally truncated to retain only total wavenumbers in the range 4–15 (4–21) prior to transformation into grid point space.

convection scheme was clearly beneficial for Z500 forecast over the Northern Hemisphere. Over Europe D+1 to D+4 forecast errors dropped by as much as about 10% of the errors seen in the control integration (with old convection). This is another example where model improvements led to both a better model climate as well as improved weather forecasts (see Rodwell and Jung, 2008, for an example associated with the African summer monsoon).

3.2.3 Linearity

So far, results from sensitivity experiments have been described in which the impact of recent model changes has been assessed for each scheme independently. This approach, however, is only efficient if non-linearity plays a secondary role, that is, the average response of a set of single model changes (linear response) is similar to the response found in an integration in which all the different model changes are incorporated simultaneously (non-linear response). Given the large number of model changes discussed in this study it is computationally prohibitive to test all combinations. However, it is worth addressing this issue for two of the most important

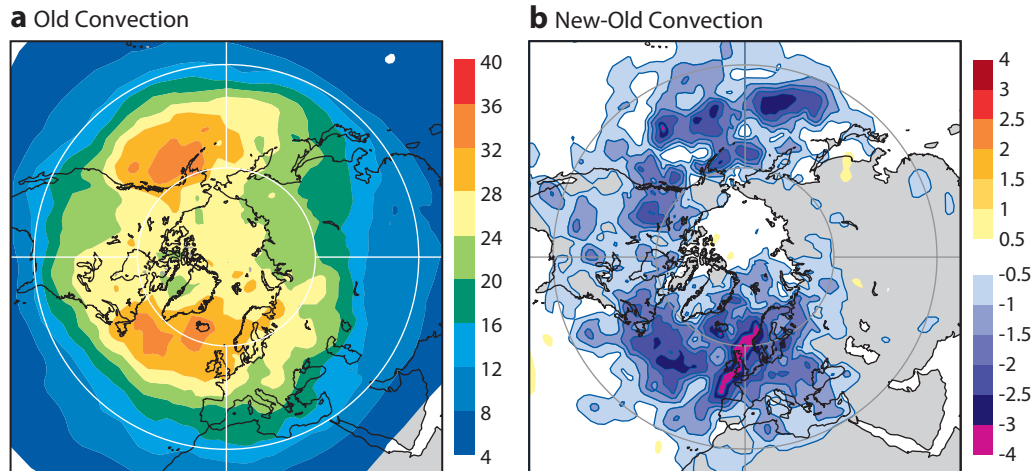


Figure 13: Mean absolute error (in m) of $D+1$ to $D+4$ Z500 forecasts: (a) control forecast with old convection, (b) difference in mean absolute error between forecasts with new and old convection. Experiments are based on version 33R1. Notice that negative values in (b) are contoured (as well as shaded).

parameterization changes, that is, that for convection (32R3) and radiation (32R1).

The linear response of the ECMWF model (version 33R1) for χ_{200} and OLR in the tropics to the new radiation and convection schemes can be inferred from Figure 14a. The linear response is obtained by averaging the two separate responses to the new radiation and convection scheme together. The non-linear response, which is obtained from a separate model integration in which both the new radiation and convection scheme are used, is shown in Figure 14b. The difference between the non-linear and linear response reflects the non-linearity of the response (Fig. 14c). The first thing to notice is that in general the linear and non-linear response are very similar suggesting that the results described in previous sections are meaningful. However, non-linear effects do play a role; especially for OLR, non-linear effects increase the strength of the response, especially over South America and the ITCZ over Africa. For χ_{200} there is some non-linearity to the north of the Equator, the cause of which is not clear. There is also some non-linearity for the Z500 response; which, however, is confined to the sub-tropics (not shown).

4 Summary and discussion

Results from a set of seasonal integrations with recent versions of the ECMWF model show that recent improvements of the physical parametrization package led to a substantial reduction of many long-standing systematic model errors. Notable improvements include the tropical hydrological cycle, and the atmospheric circulation in the Northern Hemisphere extratropics including extratropical cyclone statistics as well as the frequency of occurrence of Euro-Atlantic blocking events. Although each of the upgrades described in this study led to distinct improvements of the ECMWF model climate, the biggest single change occurred in November 2007, when the convection scheme was substantially modified.

While most of the physics changes in the ECMWF model described in this paper are beneficial there are still some issues which will need to be addressed in the near future. The observed phase speed and periodicity of the Madden-Julian Oscillation, for example, are still poorly simulated, even by the latest model version. Moreover, some aspects of the model climate have slightly deteriorated in recent years such as the Indian Summer Monsoon and near-surface zonal winds in the tropical Pacific, the latter which tends to be detrimental for seasonal

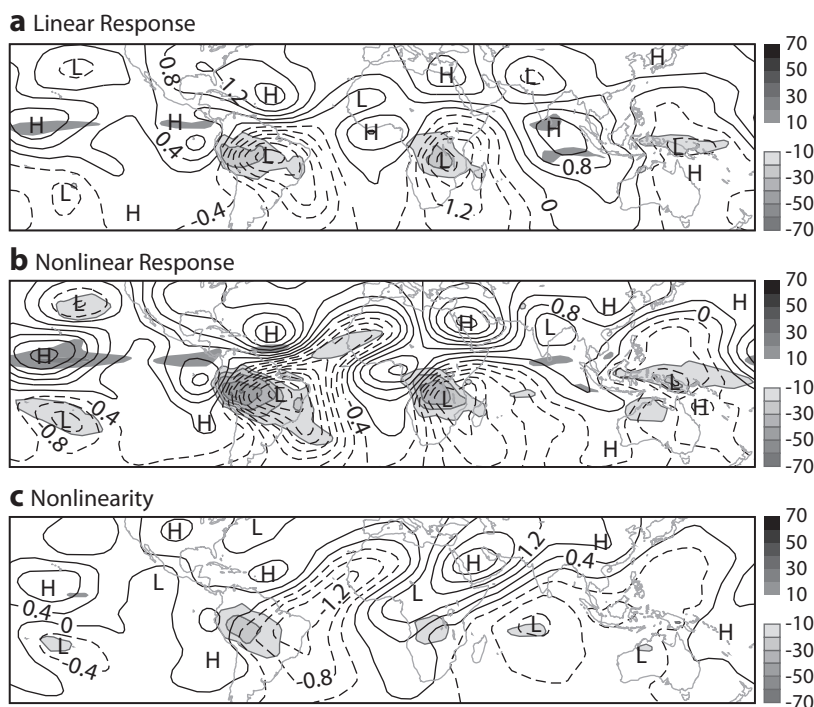


Figure 14: Mean anomalies of the velocity potential at 200 hPa (contour interval is $0.4 m^2s^{-2}$) and outgoing long wave radiation (shading in Wm^{-2}) for D+31 to D+120: (a) Mean response of two separate experiments with new convection and new radiation scheme, respectively ('linear' response), (b) response of the experiment with joint implementation of new convection and radiation scheme ('non-linear' response). (c) difference between (b) and (a) (i.e. 'non-linearity'). All results are based on seasonal integrations. Note the different contour shading for OLR compared to previous figures.

forecasts of the El Niño/Southern Oscillation phenomenon when the atmosphere model is coupled to an ocean model (Tim Stockdale, personal communication). Numerical experimentation suggests, however, that some of the deterioration of the ECMWF model climate associated with recent changes to the parametrization package can be reduced by employing a horizontal resolution higher than that used in this study (T_L159).

In order to understand the processes that led to improvements in the ECMWF model climate, a large set of additional monthly forecast experiments was carried out. By diagnosing how the model response changes as a function of lead time, it was possible to distinguish between local and remote effects. Using this seamless diagnostic approach, it turns out that the change of the radiation scheme influenced the extratropics primarily remotely from the tropics. The new convection scheme, on the other hand, has a direct impact, both in the tropics and extratropics. In the extratropics the new convection scheme reduces the strength of troughs in areas of cold air outbreaks of developed extratropical cyclones. The results of this study suggest that it is through the better simulation of diabatic processes in cold air outbreaks that the new convection scheme leads to improved short-range and medium-range forecast skill in the Northern Hemisphere extratropics.

In a previous study, Jung et al. (2006) found that the level of synoptic activity simulated by the ECMWF model is strongly dependent on the horizontal resolution employed. From this they argued that resolutions higher than T_L159 are necessary in order to obtain a realistic representation of the observed synoptic-scale systems. Their study was based on experimentation with model version 29R2. In fact, this study shows, that even at a resolution of T_L159 a more realistic level of synoptic activity can be achieved if the parameterization of subgrid-scale physical processes is improved (in this case the cloud scheme).

There are some interesting issues whose investigation goes beyond the scope of the present study. It would be

very important to understand, for example, how an increased turbulent orographic form drag increases the frequency of occurrence of Euro-Atlantic blocking events. Furthermore, it is still unclear how the new convection scheme interacts with the dynamics to produce a more realistic representation of tropical convectively-coupled waves.

Acknowledgements Dr. Antje Weisheimer kindly provided the ECMWF model script branches used to carry out the sensitivity experiments. Comments by two anonymous reviewers were very helpful for improving the quality of the paper.

References

- Adler, R. F., J. Susskind, G. Huffman, D. Bolvin, N. E., A. Chang, R. Ferraro, A. Gruber, P.-P. Xie, J. Janowiak, B. Rudolf, S. Schneider, U. Curtis, and P. Arkin, 2003: The version-2 Global Precipitation Climatology Project (GPCP) monthly precipitation analysis (1979–present). *J. Hydromet.*, **4**, 1147–1167.
- Balsamo, G., P. Viterbo, A. Beljaars, B. van der Hurk, M. Hirschi, A. K. Betts, and K. Scipal, 2009: A revised hydrology for the ECMWF model: Verification from field site to terrestrial water storage and impact in the integrated forecast system. *J. Hydrometeor.*, **10**, 623–643.
- Barker, H. W., R. Pincus, and J.-J. Morcrette, 2002: The Monte-Carlo Independent Column Approximation: Application within large-scale models. In: *Extended Abstracts, GCSS/ARM Workshop on the Representation of Cloud Systems in Large-Scale Models*, p. 10pp. Kananaskis, AB, Canada, GEWEX. Available on-line at <http://www.met.utah.edu/skrueger/gcss-2002/Extended-Abstracts.pdf>.
- Bechtold, P., M. Köhler, T. Jung, F. Doblas-Reyes, M. Leutbecher, M. Rodwell, F. Vitart, and G. Balsamo, 2008: Advances in simulating atmospheric variability with the ECMWF model: From synoptic to decadal time-scales. *Quart. J. Roy. Meteor. Soc.*, **134**, 1337–1351.
- Beljaars, A. C. M., P. Bechtold, M. Köhler, J.-J. Morcrette, A. M. Tompkins, P. Viterbo, and N. Wedi, 2004a: The numerics of physical parameterization. In: *Proceedings of ECMWF Seminar on Recent Developments in Numerical Methods for Atmospheric and Ocean Modelling*, pp. 113–134. ECMWF, Shinfield Park, Reading, Berkshire RG2 9AX, UK.
- Beljaars, A. C. M., A. R. Brown, and N. Wood, 2004b: A new parametrization of turbulent orographic form drag. *Quart. J. Roy. Meteor. Soc.*, **130**, 1327–1347.
- Boyle, J. S., 2006: Upper level atmospheric stationary waves in the twentieth century climate of the Intergovernmental Panel on Climate Change simulations. *J. Geophys. Res.*, **111**, doi:10.1029/2005JD006612.
- Brankovic, C., C. Jakob, M. Miller, A. Untch, and N. Wedi, 2002: Climate diagnostics of the ECMWF AMIP-2 simulations. Technical Report 360, Shinfield Park, Reading, Berkshire RG2 9AX, UK.
- D’Andrea, F., S. Tibaldi, M. Blackburn, G. Boer, M. Deque, M. R. Dix, B. Dugas, L. Ferranti, T. Iwasaki, A. Kitoh, D. Pope, V. Randall, E. Roeckner, D. Straus, W. Stern, H. Van den Dool, and D. Williamson, 1998: Northern Hemisphere atmospheric blocking as simulated by 15 atmospheric general circulation models in the period 1979–1988. *Clim. Dyn.*, **14**, 385–407.

- Demott, P. J., D. J. Cziczo, A. J. Prenni, D. M. Murphy, S. M. Kreidenweis, and D. S. Thomson, 2003: Measurements of the concentrations and composition of nuclei for cirrus formation. *Proc. Nat. Acad. Sci.*, **100**, 14655–14660.
- Gierens, K., 2003: On the transition between heterogeneous and homogeneous freezing. *Atmos. Chem. Phys.*, **3**, 437–446.
- Hendon, K., 1986: Streamfunction and velocity potential representation of equatorially trapped waves. *J. Atmos. Sci.*, **43**, 3038–3042.
- Hurrell, J. W., 1995: Transient eddy forcing of the rotational flow during northern winter. *J. Atmos. Sci.*, **52**, 2286–2301.
- Iacono, M. J., J. S. Delamere, E. J. Mlawer, M. W. Shephard, S. A. Clough, and W. D. Collins, 2008: Radiative forcing by long-lived greenhouse gases: Calculations with the AER radiative transfer models. *J. Geophys. Res.*, **113**, D13103, doi:10.1029/2008JD009944.
- Jung, T., 2005: Systematic errors of the atmospheric circulation in the ECMWF forecasting system. *Quart. J. Roy. Meteor. Soc.*, **131**, 1045–1073.
- Jung, T., S. K. Gulev, I. Rudeva, and V. Soloviov, 2006: Sensitivity of extratropical cyclone characteristics to horizontal resolution in the ECMWF model. *Quart. J. Roy. Meteor. Soc.*, **132**, 1839–1857.
- Jung, T., T. N. Palmer, and G. J. Shutts, 2005: Influence of a stochastic parameterization on the frequency of occurrence of North Pacific weather regimes in the ECMWF model. *Geophys. Res. Lett.*, **32**, L23811. Doi:10.1029/2005GL024248.
- Jung, T. and A. M. Tompkins, 2003: Systematic errors in the ECMWF forecasting system. Technical Report 422, ECMWF, Shinfield Park, Reading, Berkshire RG2 9AX, UK. Available at <http://www.ecmwf.int/publications/>.
- Lin, J., N. Kiladis, B. Mapes, K. Weickmann, K. Sperber, W. Lin, M. Wheeler, S. Schubert, A. Del Genio, L. Donner, S. Emori, J.-F. Guerey, F. Hourdin, P. Rasch, E. Roeckner, and J. Scinocca, 2006: Tropical intraseasonal variability in 14 IPCC AR4 climate models. Part I: Convective signals. *J. Climate*, **19**, 2665–2690.
- Lin, Y. L., R. D. Farley, and H. D. Orville, 1983: Bulk parameterization of the snow field in a cloud model. *J. Climate Appl. Meteor.*, **22**, 1065–1092.
- Lohmann, U. and B. Kärcher, 2002: First interactive simulations of cirrus cloud formed by homogeneous freezing in the ECHAM general circulation model. *J. Geophys. Res.*, **107**, 10.1029/2001JD000767.
- Louis, J. F., M. Tiedtke, and J. F. Geleyn, 1982: A short history of the PBL parameterization at ECMWF. In: *Workshop on Boundary-Layer Parametrizations*, pp. 59–79. ECMWF, Shinfield Park, Reading RG2 9AX, UK.
- Mlawer, E. J., S. J. Taubman, P. D. Brown, M. J. Iacono, and S. A. Clough, 1997: Radiative transfer for inhomogeneous atmospheres: RRTM, a validated correlated-k model for the longwave. *J. Geophys. Res.*, **102**, 16663–16682.
- Morcrette, J.-J., H. W. Barker, J. N. S. Cole, M. J. Cole, M. J. Iacono, and R. Pincus, 2008a: Impact of a new radiation package, McRad, in the ECMWF integrated forecasting system. *Mon. Wea. Rev.*, **136**, 4773–4798.

- Morcrette, J.-J., G. Mozdzynski, and M. Leutbecher, 2008b: A reduced radiation grid for the ECMWF Integrated Forecasting System. *Mon. Wea. Rev.*, **136**, 4760–4772.
- Orr, A., 2007: Evaluation of revised parameterizations of sub-grid orographic drag. Technical Report 537, ECMWF, Shinfield Park, Reading, Berkshire RG2 9AX, UK. Available at <http://www.ecmwf.int/publications/>.
- Pincus, R., H. W. Barker, and J.-J. Morcrette, 2003: A fast, flexible, approximate technique for computing radiative transfer in inhomogeneous clouds. *J. Geophys. Res.*, **108D**, 4376, doi:10.1029/2002JD003322.
- Reichler, T. and J. Kim, 2008: How well do coupled models simulate today's climate? *Bull. Amer. Meteor. Soc.*, **89**, 303–311.
- Rodwell, M. J. and T. N. Palmer, 2007: Using numerical weather prediction to assess climate models. *Quart. J. Roy. Meteor. Soc.*, **133**, 129–146.
- Rodwell, M. J. and T. Jung, 2008: Understanding the local and global impacts of model physics changes: An aerosol example. *Quart. J. Roy. Meteor. Soc.*, **134**, 1479–1497.
- Simmons, A. J. and Uppala, S. and Dee, D. and S. Kobayashi, 2007: ERA-Interim: New ECMWF reanalysis products from 1989 onwards. ECMWF Newsletter No. 110, ECMWF, Shinfield Park, Reading, Berkshire RG2 9AX, UK. Available at <http://www.ecmwf.int/publications/>.
- Sundqvist, H., E. Berge, and J. E. Kristjansson, 1989: Condensation and cloud parameterization studies with a mesoscale numerical weather prediction model. *Mon. Wea. Rev.*, **117**, 1641–1657.
- Tibaldi, S. and F. Molteni, 1990: On the operational predictability of blocking. *Tellus*, **42A**, 343–365.
- Tompkins, A. M., 2008: Cloud Parametrization. In: *Workshop on Parametrization of sub-grid physical processes*, p. pp 39. ECMWF, Shinfield Park, Reading, UK. Available from <http://www.ecmwf.int/publications>.
- Tompkins, A. M., K. Gierens, and G. Rädcl, 2007: Ice supersaturation in the ECMWF integrated forecast system. *Quart. J. Roy. Meteor. Soc.*, **133**, 53–63.
- Tompkins, A. M. and T. Jung, 2004: Influence of process interactions on MJO-like convective structures in the IFS model. In: *ECMWF/CLIVAR Workshop on Simulation and Prediction of Intra-Seasonal Variability with Emphasis on the MJO*, pp. 103–114. ECMWF, Shinfield Park, Reading RG2 9AX, UK.
- van den Hurk, B. J. J. M., P. Viterbo, A. C. M. Beljaars, and A. K. Betts, 2000: Offline validation of the ERA-40 surface scheme. Technical Report 295, ECMWF, Shinfield Park, Reading, Berkshire RG2 9AX, UK. Available at <http://www.ecmwf.int/publications/>.
- Viterbo, P. and A. C. M. Beljaars, 1995: An improved land surface parametrization scheme in the ECMWF model and its validation. *J. Climate*, **8**, 2716–2748.
- Viterbo, P., A. C. M. Beljaars, J.-F. Mahfouf, and J. Teixeira, 1999: The representation of soil moisture freezing and its impact on the stable boundary layer. *Quart. J. Roy. Meteor. Soc.*, **125**, 2401–2426.
- Wheeler, M. and G. Kiladis, 1999: Convectively coupled equatorial waves: Analysis of clouds and temperature in the wavenumber–frequency domain. *J. Atmos. Sci.*, **56**, 374–399.